

# An initial value approach to the inverse Helmholtz problem at fixed frequency

*Frank Natterer*

Institut für Numerische und  
instrumentelle Mathematik  
Universität Münster  
Einsteinstrasse 62  
D-48149 Münster, Germany

**Abstract:** *We show that the Cauchy initial value problem for the inhomogeneous Helmholtz equation is stable for spatial frequencies below a natural limit. We use initial value methods in an iterative method for the inverse problem which is very similar to ART in computerized tomography. We give numerical results for a computer generated breast phantom.*

## 1 Introduction

The inverse Helmholtz problem calls for the determination of the function  $f$  in  $\Omega \subseteq \mathbb{R}^n$  from the boundary values  $g(\theta, x) = u(x)$ ,  $x \in \partial\Omega$  of the solution  $u$  of the Helmholtz equation

$$\begin{aligned} \Delta u(x) + k^2(1 + f(x))u(x) &= 0 \\ u(x) &= e^{ikx \cdot \theta} + w(x) \end{aligned} \tag{1.1}$$

in  $\mathbb{R}^n$ , where  $w$  satisfies the Sommerfeld radiation condition. The number  $k > 0$  is the frequency of the incident plane wave with direction  $\theta \in S^{n-1}$ . We assume  $f = 0$  outside  $\Omega$ .  $g$  is measured for a single fixed frequency  $k$  and all  $\theta \in S^{n-1}$ .

The mathematical theory of this inverse problem is fairly well developed [10]. There exists an extensive literature on numerical methods. If the Born or Rytov approximation is valid, the algorithms of diffraction tomography [3] can be used. For the general case, iterative ([1], [2], [4], [8]) and direct [13] methods have been suggested.

The purpose of the present paper is to give a rigorous mathematical justification of the method already described in [12] and to demonstrate its efficacy by computer simulations.

An essential feature in [12] is the use of initial value methods for the Helmholtz equation. Initial value methods, namely the parabolic equation approximation, are also used in [1]. In contrast to [1] we work with initial value problems of second order. The stability analysis is given in §2. In §3 we describe our method for the inverse problem in a continuous setting. The necessary discretizations have been described in [12]. In §4 we report the results of the reconstruction of a breast phantom from simulated data.

## 2 The initial value problem for the Helmholtz equation

We consider the 2D Helmholtz equation

$$\frac{\partial^2 u}{\partial x_1^2} + \frac{\partial^2 u}{\partial x_2^2} + k^2(1+f)u = r \quad (2.1)$$

in the upper half plane  $x_2 > 0$ , subject to the initial conditions

$$u = g \quad , \quad \frac{\partial u}{\partial x_2} = h \quad (2.2)$$

on  $x_2 = 0$ . This problem is notoriously unstable. However, this instability is a purely high frequency phenomenon. As soon as we restrict everything to sufficiently low frequencies, this instability disappears. More precisely, let  $u_\kappa$  be a low pass filtered version of  $u$  with cut off frequency  $\kappa$ , i.e.

$$\hat{u}_\kappa(\xi_1, x_2) = \begin{cases} \hat{u}(\xi_1, x_2) & , |\xi_1| < \kappa \\ 0 & , \text{otherwise} \end{cases}$$

where  $\hat{u}$  is the Fourier transform

$$\hat{u}(\xi_1, x_2) = (2\pi)^{-1/2} \int_{-\infty}^{+\infty} e^{-ix_1 \cdot \xi_1} u(x_1, x_2) dx_1$$

of  $u$  with respect to  $x_1$ , then  $u_\kappa$  admits a perfectly reasonable estimate in terms of the initial values  $g, h$  provided  $\kappa$  is chosen properly. For  $f = 0, r = 0$  and  $\kappa < k$  this follows easily from the explicit solution

$$\hat{u}(\xi_1, x_2) = \hat{g}(\xi_1) \cos(x_2 \sqrt{k^2 - \xi_1^2}) + \frac{\hat{h}(\xi_1)}{\sqrt{k^2 - \xi_1^2}} \sin(x_2 \sqrt{k^2 - \xi_1^2}) .$$

In the following we extend this stability result to the general case.

We need the following estimate:

**Proposition 1.** *Let  $v \in C_2([0, \infty), H)$  be a solution to*

$$v'' + A(t)v = r \quad , \quad t > 0 \quad (2.3)$$

where  $A(t)$  is a linear bounded operator in the Hilbert space  $H$  with the following properties: We have  $A = A_1 + A_2$  with  $A_1^* = A_1$  and

$$\alpha_1^2(v, v) \leq (v, A_1 v) \leq \beta_1^2(v, v) \quad , \quad (2.4)$$

$$(v, A_2 v) \leq \gamma_1(v, v) \quad , \quad (2.5)$$

$$\|A_2\| \leq \beta_2 \quad (2.6)$$

with  $\alpha_1 > 0$ . Let  $\phi = (v', v') + (v, A_1 v)$ . Then,

$$\phi(t) \leq \left( \phi(0) + \int_0^t \|r(\tau)\|^2 d\tau \right) e^{(1+2\beta_2/\alpha_1 + \gamma_1/\alpha_1^2)t} . \quad (2.7)$$

**Proof:** We use the energy method see e.g. [5]. Multiplying (2.3) with  $v'$  we obtain

$$(v', v'') + (v', Av) = (v', r) . \quad (2.8)$$

Using

$$\begin{aligned} \frac{1}{2} \frac{d}{dt}(v', v') &= \operatorname{Re}(v', v'') , \\ \frac{1}{2} \frac{d}{dt}(v, A_1 v) &= \operatorname{Re}(v', A_1 v) + \frac{1}{2}(v, A_1' v) \end{aligned}$$

we can rewrite the real part of (2.8) as

$$\begin{aligned} \frac{1}{2} \frac{d}{dt}(v', v') + \frac{1}{2} \frac{d}{dt}(v, A_1 v) \\ = \operatorname{Re}(v', r) + \frac{1}{2}(v, A_1' v) - \operatorname{Re}(v', A_2 v) . \end{aligned}$$

Integrating we obtain

$$\phi(t) = \phi(0) + 2 \int_0^t \left\{ \operatorname{Re}(v', r) + \frac{1}{2}(v, A_1' v) - \operatorname{Re}(v', A_2 v) \right\} dt .$$

Cauchy-Schwarz and (2.5), (2.6) yield

$$\phi(t) \leq \phi(0) + \int_0^t \left\{ 2\|v'\|\|r\| + \gamma_1\|v\|^2 + 2\beta_2\|v'\|\|v\| \right\} dt .$$

By an appropriate use of the inequality

$$ab \leq \frac{1}{2}(\delta^2 a^2 + \delta^{-2} b^2) , \quad \delta > 0$$

we obtain

$$\begin{aligned} \phi(t) &\leq \phi(0) + \int_0^t \left\{ \|v'\|^2 + \|r\|^2 + \gamma_1\|v\|^2 + \frac{\beta_2}{\alpha_1}\|v'\|^2 + \beta_2\alpha_1\|v\|^2 \right\} dt \\ &= \phi(0) + \int_0^t \|r\|^2 dt + \int_0^t \left\{ \left(1 + \frac{\beta_2}{\alpha_1}\right) \|v'\|^2 + (\gamma_1 + \beta_2\alpha_1)\|v\|^2 \right\} dt . \end{aligned}$$

Using

$$\phi \geq \|v'\|^2 + \alpha_1^2\|v\|^2$$

we obtain

$$\phi(t) \leq c_1(t) + c_2 \int_0^t \phi(t) dt ,$$

$$c_1(t) = \phi(0) + \int_0^t \|r\|^2 dt , \quad c_2 = 1 + 2\frac{\beta_2}{\alpha_1} + \frac{\gamma_1}{\alpha_1^2} .$$

Now (2.7) follows from Gronwall's inequality (see e.g. [6], p. 24).

□

Now we can prove our stability estimate for  $u_\kappa$ .

**Theorem 2.** *Let  $f \in C^1(\mathbb{R}^2)$  and  $f = f_1 + \frac{i}{k}f_2$  with  $f_1, f_2$  real, and let  $m_\nu, M_\nu$  be constants such that*

$$-1 < m_1 \leq f_1 \leq M_1, \quad \left| \frac{\partial f_1}{\partial x_2} \right| \leq M_1, \quad |f_2| \leq M_2.$$

Then, for  $\kappa < k\sqrt{1+m_1}$ , we have

$$\|u'_\kappa(\cdot, x_2)\|^2 \leq e^{\alpha x_2} (\|h\|^2 + k^2(1+M_1)\|g\|^2 + 2\|r\|^2 + 2k^4\|f(u-u_\kappa)(\cdot, x_2)\|^2) \quad (2.9)$$

where

$$\alpha = 1 + \frac{2M_2}{\vartheta} + \frac{M_1}{\vartheta^2}, \quad \vartheta = \sqrt{1+m_1 - \left(\frac{\kappa}{k}\right)^2}.$$

**Proof:** Taking in (2.1) the Fourier transform with respect to  $x_1$  we obtain

$$\begin{aligned} (k^2 - \xi_1^2)\hat{u}(\xi_1, x_2) + \frac{\partial^2}{\partial x_2^2}\hat{u}(\xi_1, x_2) + (2\pi)^{-1/2}k^2 \int_{-\infty}^{+\infty} \hat{f}(\xi_1 - \eta_1, x_2)\hat{u}(\eta_1, x_2)d\eta_1 \\ = \hat{r}(\xi_1, x_2). \end{aligned}$$

We consider this equation only for  $|\xi_1| \leq \kappa$  and decompose the integral accordingly, i.e.

$$\begin{aligned} (k^2 - \xi_1^2)\hat{u}_\kappa(\xi_1, x_2) + \frac{\partial^2}{\partial x_2^2}\hat{u}_\kappa(\xi_1, x_2) + (2\pi)^{-1/2}k^2 \int_{-\infty}^{+\infty} \hat{f}(\xi_1 - \eta_1, x_2)\hat{u}_\kappa(\eta_1, x_2)d\eta_1 \\ = \hat{r}(\xi_1, x_2) + \hat{\varepsilon}(\xi_1, x_2), \quad \hat{\varepsilon}(\xi_1, x_2) = -(2\pi)^{-1/2}k^2 \int_{|\eta_1| \geq \kappa} \hat{f}(\xi_1 - \eta_1, x_2)\hat{u}(\eta_1, x_2)d\eta_1. \end{aligned}$$

Obviously,

$$\varepsilon = -k^2 f(u - u_\kappa).$$

For fixed  $\xi_1$  we rewrite the last equation for  $\hat{u}_\kappa$  as

$$\hat{u}_\kappa''(x_2) + A(x_2)\hat{u}_\kappa(x_2) = \hat{r}(x_2) + \hat{\varepsilon}(x_2) \quad (2.10)$$

In order to apply Proposition 1 to (2.9) we only have to find the constants in (2.4 - 2.6) for the operator  $A$  from (2.10). We have

$$\begin{aligned} (A\hat{u}, \hat{v}) &= ((k^2 - \xi_1^2)\hat{u}, \hat{v}) + (2\pi)^{-1/2}k^2 \int_{-\infty}^{+\infty} (\hat{f} \star \hat{u})\bar{\hat{v}}d\xi_1 \\ &= ((k^2 - \xi_1^2)\hat{u}, \hat{v}) + k^2 \int_{-\infty}^{+\infty} \widehat{f\hat{u}}\bar{\hat{v}}d\xi_1 \\ &= ((k^2 - \xi_1^2)\hat{u}, \hat{v}) + k^2 \int_{-\infty}^{+\infty} f\hat{u}\bar{\hat{v}}dx_1 \end{aligned}$$

where we have used Parseval's relation. Writing  $f$  as  $f_1 + \frac{i}{k}f_2$  it readily follows that

$$(A_1 \hat{u}, \hat{u}) = ((k^2 - \xi_1^2) \hat{u}, \hat{u}) + k^2 \int_{-\infty}^{+\infty} f_1 |u|^2 dx_1 ,$$

$$(A_2 \hat{u})^\sim = ik f_2 u .$$

From these relations we easily read

$$\alpha_1^2 = k^2 - \kappa^2 + k^2 m_1 , \quad \beta_1^2 = k^2(1 + M_1) , \quad \gamma_1 = k^2 M_1 , \beta_2 = k M_2 .$$

Inserting this into (2.7) and using

$$\|\hat{u}'_\kappa(\cdot, x_2)\|^2 \leq \phi(x_2) \leq \|\hat{u}'_\kappa(\cdot, x_2)\|^2 + k^2(1 + M_1) \|\hat{u}_\kappa(\cdot, x_2)\|^2$$

yields (2.9). □

The estimate of Theorem 2 makes sense only if  $u - u_\kappa$  is small in some sense. In the next theorem we show that this is in fact the case for the scattered wave  $w$  from (1.1) with  $\theta = \begin{pmatrix} 0 \\ 1 \end{pmatrix}$ . For  $w$  we have the Lippmann-Schwinger equation

$$w(x) = \frac{-i}{4} k^2 \int_{\mathbf{R}^2} H_0(k|x - x'|) f(x') (e^{ikx'_2} + w(x')) dx'$$

with the Hankel function of the first kind  $H_0$ . Taking the Fourier transform with respect to  $x_1$  we obtain

$$\begin{aligned} & \hat{w}(\xi_1, x_2) \\ &= -\frac{i}{4\sqrt{2\pi}} k^2 \iint \int H_0(k\sqrt{(x_1 - x'_1)^2 + (x_2 - x'_2)^2}) e^{-i\xi_1 x_1} dx_1 \\ & \quad (e^{ikx'_2} + w(x'_1, x'_2)) f(x'_1, x'_2) dx'_1 dx'_2 . \end{aligned}$$

The  $x_1$  integral can be evaluated as follows. With  $a(\xi) = \sqrt{k^2 - \xi^2}$  we have

$$H_0(k\sqrt{u^2 + v^2}) = \frac{-i}{4\pi} \int e^{i(|u|a(\xi) + v\xi)} \frac{d\xi}{a(\xi)} ,$$

see e.g. [9], p. 123. Hence

$$\begin{aligned} \int H_0 \left( k\sqrt{(x_1 - x'_1)^2 - (x_2 + x'_2)^2} \right) e^{-i\xi_1 x_1} dx_1 &= \frac{-i}{4\pi} \int \int e^{i(|x_2 - x'_2|a(\xi) + (x_1 - x'_1)\xi) - i\xi_1 x_1} \frac{dx_1 d\xi}{a(\xi)} \\ &= \frac{-i}{2} \int e^{i(|x_2 - x'_2|a(\xi) - x'_1 \xi)} \delta(\xi - \xi_1) \frac{d\xi}{a(\xi)} \\ &= -\frac{i}{2} e^{i(|x_2 - x'_2|a(\xi_1) - x'_1 \xi_1)} \frac{1}{a(\xi_1)} . \end{aligned}$$

It follows that

$$\begin{aligned} & \hat{w}(\xi_1, x_2) \\ &= \frac{k^2}{8a(\xi_1)} \int \int e^{i(|x_2-x'_2|a(\xi_1)-x'_1\xi_1)} \left( e^{ikx'_2} + w(x'_1, x'_2) \right) f(x'_1, x'_2) dx'_1 dx'_2 . \end{aligned}$$

Now assume that the straight line  $x'_2 = x_2$  misses  $\text{supp}(f)$  by the quantity  $\varepsilon > 0$  and  $\xi_1 > k$ . Then,

$$|\hat{w}(\xi_1, x_2)| \leq \frac{k^2}{8\sqrt{\xi_1^2 - k^2}} e^{-\varepsilon\sqrt{\xi_1^2 - k^2}} (1 + \|w\|_\infty) \|f\|_1 .$$

Hence we have for arbitrary  $\theta$ :

**Theorem 3.** *Let  $w$  be the scattered wave for incident direction  $\theta$ , and let  $L$  be a straight line perpendicular to  $\theta$  which misses the support of  $f$ . Then, the Fourier transform of  $w$  along  $L$  decays exponentially beyond  $k$ .*

We shall apply Theorem 2 with  $m_1$  negative but close to zero (typically  $m_1 = -0.01$ ). Then, Theorem 2 requires  $\kappa$  to be slightly smaller than  $k$ , while, according to Theorem 3,  $u - u_\kappa$  in Theorem 2 is small if  $\kappa$  is slightly bigger than  $k$ . In practice this conflict did not cause any problems. With  $\kappa = 0.99k$  we observed both stability and accuracy.

### 3 The inversion method

We consider the case  $n = 2$ . Assume that  $\Omega$  is the ball of radius  $\rho$  centered at the origin. Let the scattered field  $w_j$  be measured on  $\partial\Omega$  for  $p$  directions  $\theta_j$ . We first extend  $w_j$  to the exterior of  $\Omega$ . Since  $w_j$  satisfies there the homogeneous Helmholtz equation  $\Delta w_j + k^2 w_j = 0$ , this is easily done by expanding  $w_j(x)$  for  $|x| > \rho$  as

$$w_j(r \cos \varphi, r \sin \varphi) = \sum_{\ell} c_{\ell} e^{i\ell\varphi} H_{\ell}(kr)$$

with  $H_{\ell}$  the first kind Hankel function of order  $\ell$ . The coefficients  $c_{\ell}$  are readily obtained from the data by

$$c_{\ell} = \frac{1}{2\pi H_{\ell}(k\rho)} \int_0^{2\pi} w_j(\rho \cos \varphi, \rho \sin \varphi) d\varphi .$$

Now let  $Q_j$  be the square circumscribed to  $\Omega$ , two of its edges, named  $\Gamma_j$ , parallel to  $\theta_j$ . The other edges are denoted by  $\Gamma_j^-$ ,  $\Gamma_j^+$  with  $\theta_j$  pointing from  $\Gamma_j^-$  to  $\Gamma_j^+$ . We define an operator  $R_j : L_2(\Omega) \rightarrow L_2(\Gamma_j^+)$  by solving the initial value problem

$$\begin{aligned} \Delta w + k^2(1 + f)w &= -k^2 f e^{ikx \cdot \theta} \quad \text{in } Q_j , \\ w &= w_j , \quad \frac{\partial w}{\partial \nu} = \frac{\partial w_j}{\partial \nu} \quad \text{on } \Gamma_j^- , \quad w = w_j \quad \text{on } \Gamma_j \end{aligned}$$

and putting  $R_j(f) = w$  on  $\Gamma_j^+$ . We also put  $g_j = w_j|_{\Gamma_j^+}$ .

Now we have to solve the nonlinear system

$$R_j(f) = g_j, \quad j = 1, \dots, p$$

for  $f$ . We do this by an ART type algorithm.

With  $f^0$  an initial approximation to  $f$  we compute a new approximation  $f^1$  by

$$\begin{aligned} f_0 &= f^0, \\ f_j &= f_{j-1} + \gamma R_j^*(f_{j-1})(g_j - R_j(f_{j-1})), \quad j = 1, \dots, p \\ f^1 &= f_p. \end{aligned}$$

$\gamma$  is a relaxation parameter.

$R_j^*$  can be evaluated by solving an initial value problem with initial values on  $\Gamma_j^+$ . This can be done by the usual five point finite difference star, combined with filtering along the grid lines perpendicular to  $\theta_j$ . For details see [12].

## 4 Numerical experiment

We did reconstructions from data obtained from a computer generated breast phantom which has been patterned after a phantom created by Borup et al. [1]. With  $c$  the sound speed in the breast tissue,  $c_0 = 1500 \frac{m}{sec}$  the sound speed in the surrounding water, and  $\alpha$  the attenuation coefficient in the breast tissue we have

$$f = \frac{c_0^2}{c^2} - 1 - i \frac{2\alpha c_0}{kc}, \quad \omega = c_0 k. \quad (4.1)$$

The phantom is made up of four different kinds of tissue: fat, glandular tissue, tumor, and cyst. The values of  $c$  and  $\alpha$  (at 1MHZ) are

tissue	$c[\frac{m}{sec}]$	$\alpha[\frac{db}{m}]$	$Re f$	$Im f$
fat	1458	41	0.058	-9.4/k
glandular tissue	1519	80	-0.025	-18.4/k
tumor	1564	118	-0.080	-27.2/k
cyst	1568	10	-0.084	-2.3/k

The value of  $\alpha$  in column 2 have to be converted to those in formula (4.1) by dividing with the factor  $20 \log_{10}(e)$ , yielding  $\alpha$  in units  $[\frac{1}{m}]$ . Therefore,  $k$  in column 4 is in units of  $[\frac{1}{m}]$ , too.

We generated data by solving the forward problem with the initial value method, assuming the backscatter to be zero. We worked on a  $128 \times 128$  grid, using  $p = 128$  equally spaced directions in  $[0, 2\pi)$ . The frequency of the irradiating plane waves was 1MHZ, i.e.  $\omega = 2\pi \cdot 10^6 \text{ sec}^{-1}$ , hence  $k = 4189m^{-1}$ .

The condition for the Born approximation to hold is

$$R|f| \ll \frac{2\pi}{k}$$

where  $R$  is the Radon transform. This is a slight generalisation of the condition given by Kak and Slaney [7]. It is obviously far from being satisfied. As has been discussed in [12], we can't use 0 as initial approximation in this case. We used the reconstruction for the smaller value  $k = 1000 \text{ m}^{-1}$  instead which can be computed starting out from 0. A smoothed version of the initial approximation thus obtained is shown in Fig. 2.

The reconstruction after 6 sweeps is shown in Fig. 3. The total computation time on a SPARC 20 was 5 minutes. The value of  $\gamma$  has been chosen in the following way. First we determined in [11] the asymptotic value  $1/(\rho k^2)$  of the operator  $(R'_j(0)R_j^{*'}(0))^{-1}$  for large  $k$ . Then we put  $\gamma = \gamma'/(\rho k^2)$  where, in agreement with the convergence properties of the Kaczmarz procedure,  $0 < \gamma' < 2$ . We used  $\gamma' = 0.5$ .

## References

1. Borup, D.T. - Johnson, S.A. - Kim, W.W. - Berggren, M.J.: Nonperturbative diffraction tomography via Gauss-Newton iteration applied to the scattering integral equation, *Ultrasonic Imaging* **14**, 69-85 (1992).
2. Colton, D. - Monk, P.: A modified dual space method for solving the electromagnetic inverse scattering problem for an infinite cylinder, *Inverse Problems* **10**, 87-108 (1994).
3. Devaney, A.J.: A filtered backpropagation algorithm for diffraction tomography, *Ultrasonic Imaging* **4**, 336-350 (1982).
4. Gutman, S. - Klibanov, M.: Regularized Quasi-Newton method for inverse scattering problems, *Math. Comput. Modelling* **18**, No. 1, pp. 5-31, Pergamon Press Ltd. (1993).
5. Hahn, W.: *Stability of motion*. Springer 1967.
6. Hartman, P.: *Ordinary differential equations*, Wiley 1964.
7. Kak, A.C. - Slaney, M.: *Principles Computerized Tomographic Imaging*, IEEE Press, New York 1987.
8. Kleinman, R.E. - van den Berg, P.M.: A modified gradient method for two-dimensional problems in tomography, *J. Comp. Appl. Math.* **42**, 17-35 (1992).
9. Morse, P.M. - Feshbach, H.: *Methods of theoretical physics*, McGraw-Hill 1953.
10. Nachman, A.I.: Global uniqueness for a two-dimensional inverse boundary value problem. *Department of Mathematics, Preprint Series*, Number **19**, University of Rochester (1993).
11. Natterer, F.: Finite Difference Methods for Inverse Problems, in Ang, D.D. et al. (eds.): *Inverse Problems and Applications to Geophysics, Industry, Medicine and Technology. Publications of the HoChiMinh City Mathematical Society*, **Vol. 2**, 1995.
12. Natterer, F. - Wübbeling, F.: A propagation - backpropagation method for ultrasound tomography. *Inverse Problems* **11**, 1225-1232 (1995).
13. Stenger, F. - O'Reilly, M.: Sinc inversion of the Helmholtz equation without computing the forward solution, Preprint, Department of Computer Science, University of Utah, Salt Lake City, Utah 84112.

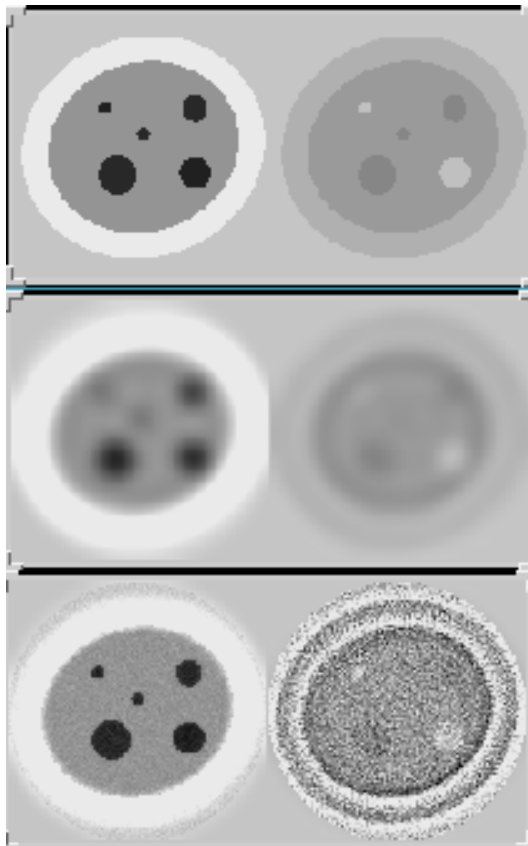


### Figure captions

- Fig. 1 (top)** : Breast phantom. Real part left, imaginary part right. Since the imaginary part is much smaller than the real part it has been scaled. The location of the 3 tumors and 2 cysts is clear from the real part, while they can be distinguished by looking at the imaginary part.
- Fig. 2 (middle)** : Initial approximation which has been computed from data corresponding to  $k = 1000 \text{ m}^{-1}$  using 0 as initial approximation.
- Fig. 3 (bottom)** : Reconstruction after 6 sweeps with  $\gamma' = 0.5$ .